(e)ISSN 2656-8896 (p)ISSN 2656-890X
Journal of Infrastructure and Facility Asset Management – Vol. 7, Issue 1, January 2025

Planning of Alternative Embankment Reinforcement on the Roadway. Case Study: Landslide on the Bypass Road of Lombok International Airport - Mandalika Section Km 10+415 to 10+519

Panji Ageng Ichtiar[1,a], Mohamad Khoiri[2,b], Dwa Desa Warnana[3,c] & Herlambang Zulfikar[4,d]

[1]Magister Student, Departement of Civil Engineering, Institut Teknologi Sepuluh November (ITS), Surabaya
[2]Departement of Civil Engineering, Institut Teknologi Sepuluh November (ITS), Surabaya
[3]Departement of Geophysics, Institut Teknologi Sepuluh November (ITS), Surabaya
[4]Head of the National Road Implementation Work Unit for Region 1, West Nusa Tenggara Province

Correspondent : [a]Panji.Ichtiar@pu.go.id, [b]mkhoiri@ce.its.ac.id, [c]dwa_desa@yahoo.co.uk, [d]herlambang_zul@yahoo.com

ABSTRACT

The Lombok International Airport – Mandalika Bypass Road experienced a landslide at KM 10+415 to 10+519 in February 2023 during heavy rainfall. The landslide is estimated to have occurred due to the saturation of the embankment caused by groundwater flow and rainwater infiltration. The proposed reinforcement includes the use of foam mortar with thickness variations of 2m, 4m, and 6m, with or without subdrain. Another proposal involves using Rigid Inclusions in the form of controlled modulus columns (CMC) with column spacing variations of 2ø, 3ø, and 4ø, with or without subdrain. Numerical analysis of the safety factor (SF) and deformation (Uy) was conducted using the Plaxis 2D program, both for the initial condition and after reinforcement. In general, the SF and deformations (Uy) for all reinforcement variations meet the reinforcement criteria, i.e., SF > 1.5 and deformations (Uy) < 2cm. The smallest SF of 1.579 was obtained with 4m thick foam mortar with subdrain. The largest deformations (Uy) of 1.656 was found with 2ø column spacing CMC without subdrain. The most effective Stress Reduction Ratio of 0.13 was achieved with 2ø column spacing CMC without subdrain. The influence of the subdrain is not significant because the landslide surface did not reach the groundwater table.

Keyword : safety factor, deformation (uy), foam mortar, rigid inclusions, subdrain

INTRODUCTION

The Lombok International Airport – Mandalika Bypass Road, based on the Decree of the Minister of Public Works and Public Housing Number 430/KPTS/M/2022 dated April 28, 2022, concerning the Designation of Segments in the Primary Road Network According to Their Function as Primary Arterial Road (JAP) and Primary Collector Road – 1 (JKP – 1), is a National Road with Segment Number 75 050, spanning a length of 17.36 km. According to its function, it is a Primary Arterial Road. This road connects Lombok International Airport with the Mandalika Special Economic Zone in southern Lombok, which includes the MotoGP circuit.

The Directorate General of Highways, Ministry of Public Works and Public Housing, through the National Road Implementation Center of West Nusa Tenggara, completed the construction of the BIL – Mandalika Bypass Road in December 2022. The landslide occurred at STA 10+415 to 10+519 between February and July 2023, with a deformations (Uy) of approximately 179 cm. Prior to the landslide, cracks had appeared on the road surface starting in February 2023, but these cracks were promptly sealed. When the investigation was conducted in August 2024, an additional deformations (Uy) of 5 cm was observed. The location of the BIL – Mandalika Bypass Road is shown in Figure 1.

Figure 1. Road section Bypass BIL – Mandalika (Satker P2JN NTB, 2024)

The research location is shown in Figure 2. namely on the BIL - Mandalika Bypass Road Section KM 10 + 415 - KM 10 + 519 experiencing landslides that form a crown or circular arc curve with the direction of the landslide heading east or towards Embung.

Figure 2. Landslide Surface on the road section Bypass BIL – Mandalika Km 10+415 s.d. Km 10+519 (Satker P2JN NTB, 2024)

LITERATURE STUDY

Lanslide Theory

According to (Das, 2008), an open ground surface that forms an angle with the horizontal is called an uncontrolled slope. The slope can be natural or artificial. If the ground surface is not flat, the gravitational force components will cause the soil to move downward. If the gravitational components are large enough, slope failure can occur. This means that the mass of soil can slide downward. The driving force of the soil mass is greater than the resistance, which is the shear strength of the soil along the failure surface. (Das, 2011) classifies landslide types into six categories, which are:

1. Falls, the collapse of part of the rock mass on a steep slope;
2. Topples, occurring due to forward rotation of one or more units around a pivot point below, caused by gravity or forces exerted by adjacent units;

3. Slides, shear strain and soil movement on several soil surfaces. This movement may have a forward direction, starting from local shear failure and then progressing into a landslide, with the sliding soil breaking apart;
4. Spreads, the lateral or outward spreading of soil due to shear failure or tensile failure along nearly horizontal soil layers;
5. Flows, a condition where the soil behaves like a thick fluid due to the velocity and displacement within the soil mass. The slip surface is usually not visible, and it occurs rapidly;
6. Complex Landslides occur when the soil movement is a combination of several types of soil movements.

Foam Mortar

(Wartoyo, 2022) Foam mortar is a material resembling concrete that consists of a mixture of sand, cement, water, and foam liquid (foam agent), and functions as a substitute for embankment material. The use of foam mortar as a replacement for regular soil embankment aims to lighten the weight of the embankment because foam mortar is lighter than regular soil. With its lighter weight, it is expected that the driving forces acting on the embankment will be smaller, thus improving the safety factor of the embankment's stability.

The Ministry of Public Works and Public Housing, through the Technical Planning Guidelines for Lightweight Foam Mortar Embankment Material for Road Construction, Number 42/SE/M/2015, Year 2015, states that the use of lightweight foam mortar material refers to Table 1.

Table 1. Foam mortar material parameter (Kementerian PUPR, 2015)

Maximum ɣ dry (gr/cm^3)	Minimum compressive strength		Usage
	kPa	Kg/cm^2	
0.8	2000	20	foundation or base layer
0.6	800	8	sub-foundation layer

According to the research by (Hidayat, 2016), the use of lightweight material with foam mortar as fill material over a foundation soil with low bearing capacity provides several advantages, including lower deformation compared to conventional embankments (Wartoyo, 2022). The SF criteria and deformations (Uy) for using foam mortar as embankment material are presented in Table 2 and Table 3.

Table 2. SF minimum foam mortar (Kementerian PUPR, 2015)

Road grade	Safety Factor
I	1.4
II	1.4
III	1.3
IV	1.3

Table 3. Foam Mortar embankment deformation (Uy) criteria (Kementerian PUPR, 2015)

Road Grade	The Required Doformation (Uy) During Construction s/s_{tot}	Decrease Speed After Construction (mm/tahun)
I	>90%	<20
II	85%	<25
III	80%	<30
IV	75%	<30

Note: s is the amount of deformation during the contruction period s_{tot} is the total expected deformation

Rigid Inclusions

Rigid Inclusions originate from the arching effect theory, which is a theory of load distribution. Rigid Inclusions is a ground improvement method developed by Menard Soiltreatment in the 1990s. The main idea behind Rigid Inclusions, one of which is the Controlled Modulus Column (CMC), is to transfer loads to the soil by inserting rigid columns into soft soil to improve deformations (Uy) and bearing capacity. These rigid columns are filled with concrete and are without reinforcement, capped with small pile caps. Then, above the pile cap, a load transfer layer, or Load Transfer Platform (LTP), is provided, consisting of aggregate or sand.

Menard, as explained in (Endah, 2018), describes the arching effect theory, which states that the load from the surface is transferred to the CMC through the LTP, while the soil between the CMCs only receives 10% - 30% of the total stress from the surface. The load distribution scheme is shown in Figure 3.

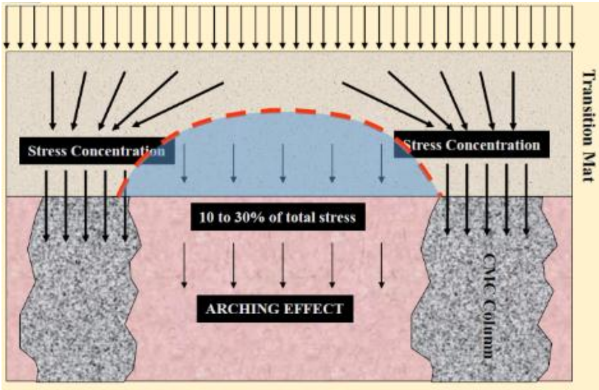

Figure 3. The load distribution scheme for Rigid Inclusions based on the arching effect theory (Menard in Endah, 2018).

The arching effect phenomenon can be observed using the stress comparison (stress reduction ratio/SRR). The stress reduction ratio value is the ratio of the stress in the soil between the columns and the external load applied. For the soil stress value between the columns at an elevation below the LTP layer, the output results from modeling analysis using Plaxis 2D are used, considering the nearest stress point. The stress reduction ratio (SRR) has a value range from 0 to 1. A value of 0 represents a perfect arching effect, while a value of 1 represents no arching effect in the soil reinforcement system. The SRR value can be calculated using the equation below.

$$SRR = \frac{\sigma s}{\sigma p} \quad \ldots(1)$$

Where:

SRR = Stress Reduction Ratio

σs = The soil pressure at the observation point below the LTP between the CMC columns.

σp = The pressure due to the external load.

The SF requirements follow SNI 8460:2017 and the Minister of Public Works and Public Housing No. 44/SE/M/2015, which state that the Slope SF and Global SF for various types of reinforcement must be > 1.5, and the deformation (Uy) must be < 2 cm.

Subdrain

According to (Moulton, 1980), highway subdrains can function as a control for the groundwater table elevation, specifically eliminating and/or controlling the flow of groundwater. It has the same function as infiltration control, which aims to remove water that flows into the roadbed. Figure 4 shows the function of subdrains in lowering the groundwater table.

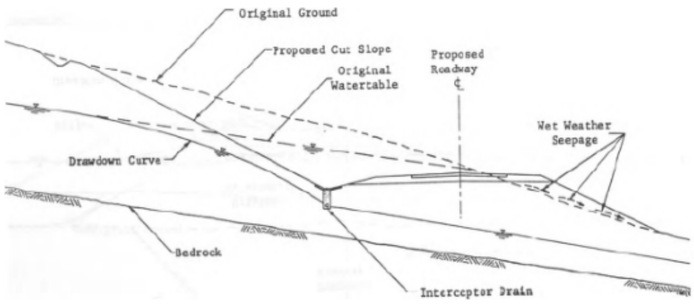

Figure 4. The function of subdrains to lower the groundwater table (Moulton, 1980).

RESEARCH METHODE

After obtaining secondary data from soil testing by PT. Jepari Jaya in July 2024 and primary data in August 2024, a numerical analysis was conducted for the initial condition when deformations (Uy) occurred, using combined soil parameters from the secondary and primary data. If the resulting SF does not match field conditions, a back analysis is performed to adjust the soil parameters. The soil parameters from the back analysis are then used in the reinforcement modeling using foam mortar and rigid inclusions with controlled modulus columns (CMC) with the following variations:

1. Foam mortar thickness of 2m with subdrain;
2. Foam mortar thickness of 4m with subdrain;
3. Foam mortar thickness of 6m with subdrain;
4. Foam mortar thickness of 2m without subdrain;
5. Foam mortar thickness of 4m without subdrain;
6. Foam mortar thickness of 6m without subdrain;
7. CMC column spacing of 2ø with subdrain;
8. CMC column spacing of 3ø with subdrain;
9. CMC column spacing of 4ø with subdrain;
10. CMC column spacing of 2ø without subdrain;
11. CMC column spacing of 3ø without subdrain;
12. CMC column spacing of 4ø without subdrain.

Then, SF and deformation (Uy) analyses are performed for these variations.

DATA COLLECTION

The secondary data sources consist of two: from P2JN NTB after the landslide event, and from PT. Jepari Jaya in July 2024. The primary data refers to soil parameter testing conducted in August 2024. The P2JN NTB data provides the stratigraphy and the groundwater table elevation, while the PT. Jepari Jaya data provides the NSPT values, cohesion, and shear angle, with other soil parameters being sourced from the primary data. Figure 5 shows the stratigraphy formed from BH1, BH2, and BH3 testing by P2JN NTB on May 6, 2023.

To obtain the values of Elastic Modulus (E) and Poisson's Ratio (v) for input into Plaxis 2D, correlations between soil type and soil consistency with E and v are used (Bowles, 1997). Table 4 displays the values of E and v used for Plaxis 2D input.

Table 6. The correlation between soil parameters, Elastic Modulus (E) and Poisson's Ratio (v), is based on soil type and consistency (Bowles,1997)

Soil type	Drain type	E	v	c (kN/m^2)	ϕ (°)	ɣ unsat (kN/m^3)	ɣ sat (kN/m^3)	k (m/day)
Gravelly sand with brown silt	Mohr Coulomb Drained	5000	0.3	15.7	20	15.7	18.8	4.47
Silty sand with brown gravel	Mohr Coulomb Drained	15000	0.3	18.63	23	14	18.1	0.49
Black silty clay	Mohr Coulomb UndrainedA	8000	0.35	33.3	14	13.1	17.6	0.000133
Clayeyi grevel with silt	Mohr Coulomb Drained	100000	0.3	34.2	33	15.7	19.3	0.864
Weathered Breccia Rock	Mohr Coulomb Drained	100000	0.3	8	17.47	16.1	18.87	0.864

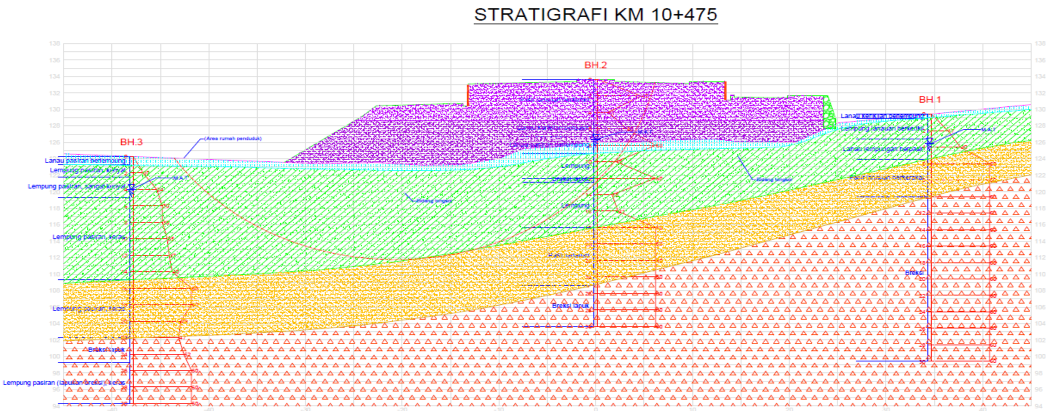

Figure 4. The stratigraphy formed from BH1, BH2, and BH3 testing conducted by P2JN NTB on May 6, 2023

RESEARCH ANALISIS

Initial Conditions

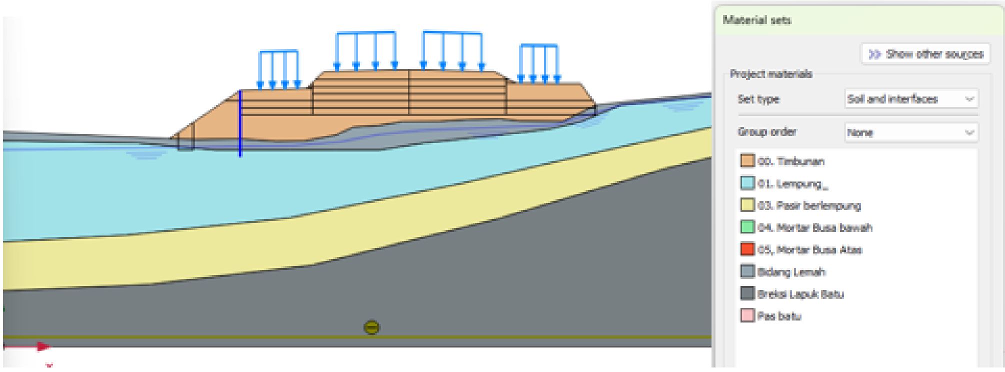

Figure 5. Geometric Modeling of STA 10+475 BIL – Mandalika Road Segment

In the initial modeling, a deformations (Uy) of the road surface (uy) of 0.009577 m or 0.9 cm and a safety factor (SF) of 1.886 were obtained. However, this did not match the actual field conditions, where deformations (Uy) had already occurred. Therefore, a back-analysis was performed to determine the soil parameters that align with the field conditions.

After conducting the back analysis, the deformations (Uy) that occurred was 0.01016 m or 1.016 cm, and the SF was 0.9395, which corresponds to the field conditions observed in August 2024. The deformations (Uy) area and the obtained SF after the back analysis process are shown in Figure 6.

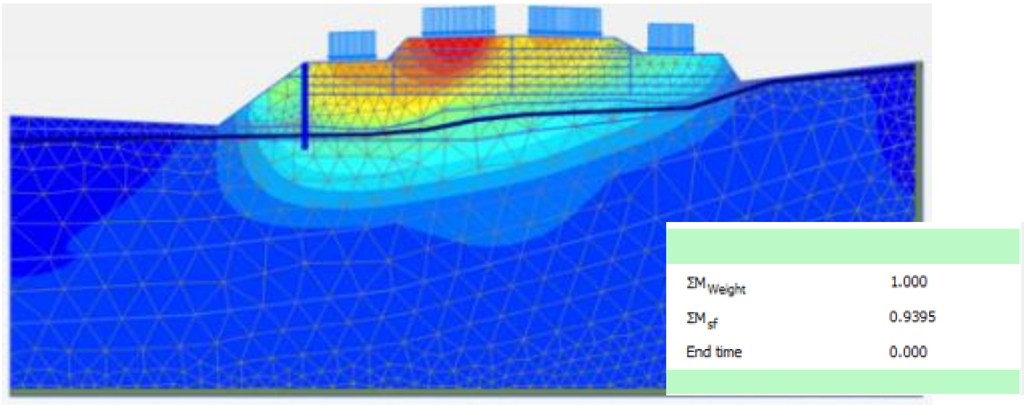

Figure 6. The deformations (Uy) area and the SF obtained after the back analysis process.

The reason for the back analysis at this stage is the discrepancy between the initial SF condition, which was 1.886, and the field conditions where a deformations (Uy) of 5 cm had already occurred in August 2024. The adjustment of parameters was made to the embankment soil layer, where the borehole test results showed relatively low NSPT values ranging from 4 to 15. This indicates that the embankment (gravelly sand and brown silt) had experienced a loss of compaction. As a result, the values of C' and Ø' for the embankment soil were adjusted from the original values of C' = 15.7 kN/m² and Ø' = 20° to C' = 5.5 kN/m² and Ø' = 15°.

Reinforcement Analysis

The subdrain will be placed on the outer side of the frontage road on the right-hand side toward Mandalika, beneath the surface drainage system. The dimensions of the subdrain are 3 meters in depth, 1 meter in width, and 150 meters in length, with two perforated pipes of 11inch diameter placed at the bottom of the subdrain.

The variations of reinforcement using foam mortar thickness and CMC column spacing are shown in Figure 7.

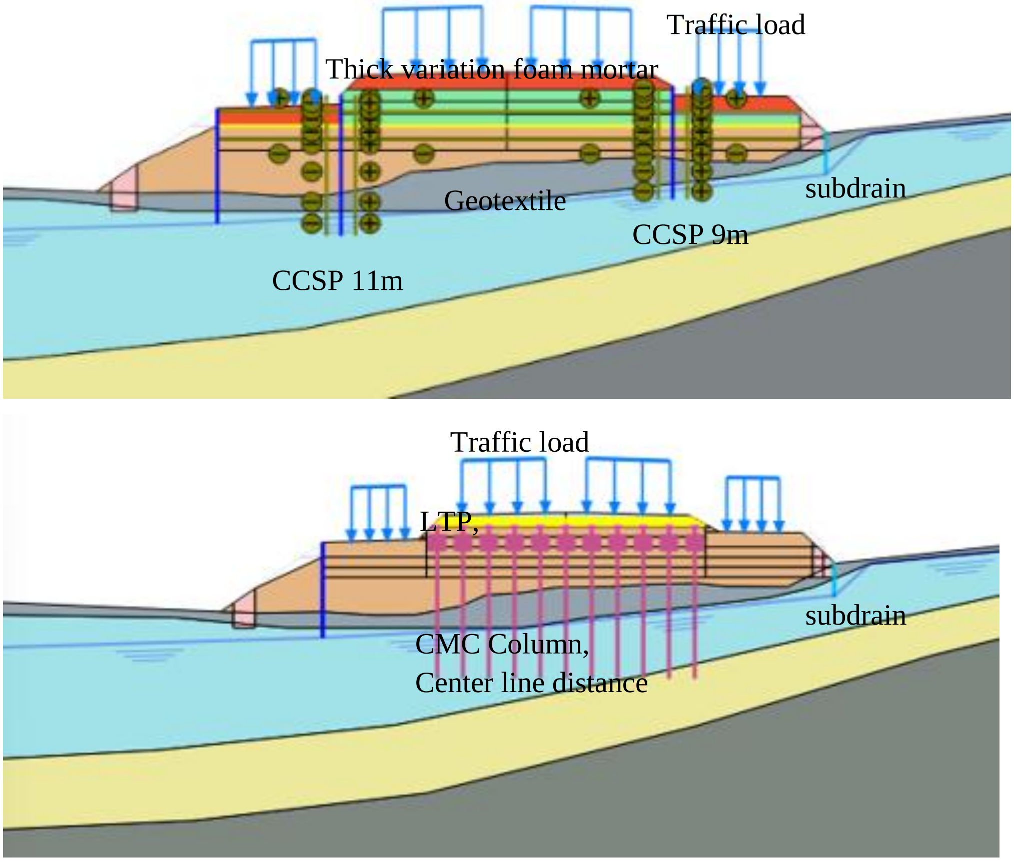

Figure 7. Geometry of Foam Mortar Thickness Variations, CMC Column Spacing Variations, and Subdrain Usage

The traffic load according to the Ministry of Public Works and Housing (Kementerian PUPR, 2015) for class I roads is 15 kPa. The geotextile used for both foam mortar reinforcement and CMC reinforcement has a tensile strength of T = 100 kN and a strain (ε) of 5%, resulting in an EA value of 2000 kN/m². Meanwhile, for the LTP sand, it is planned to have a medium-dense density with properties shown in Table 7.

Table 7. LTP sand medium dense

Material type	**Drain type**	**E**	**v**	**c (kN/m^2)**	**ϕ (^{o})**	**ɣ unsat (kN/m^3)**
LTP sand	Mohr Coulomb Drained	100000	0.3	5	35	17

The use of CCSP is related to the method of applying foam mortar reinforcement, where the road body must not be completely closed during construction work. The CCSP used is a product from PT. Wika Beton, type CCSP W 500. The material properties of the foam mortar are provided in Table 1.

For the CMC columns, it is planned to have a diameter of 0.6 m and a length of 15 m. The capping dimensions are 0.7 m x 0.7 m x 0.2 m, with a compressive strength (fc') for both the column and capping of 30 MPa. The end resistance (Qp/Fmax) is 385.16 kN, the frictional resistance (Qs/Tmax) is 114 kN/m, and the elastic modulus (E) is 25,742,960.2 kN/m².

The SF (Safety Factor) and deformations (Uy) values for the 12 variations of reinforcement are shown in Table 8.

Table 8. SF (Safety Factor) and Deformations (Uy) from Various Reinforcement Variations

Reinforcement alternative	Thicknes of foam mortar (m) / distance of column (ø)	Safety factor	Deformation Uy (cm)
Foam Mortar + Subdrain	2	1.59	0.7893
	4	1.579	0.5823
	6	1.599	0.3554
Mortar Busa	2	1.593	0.8132
	4	1.583	0.6102
	6	1.599	0.3826
CMC + Subdrain	2	1.601	1.607
	3	1.594	1.255
	4	1.6	1.184
CMC	2	1.592	1.656
	3	1.583	1.304
	4	1.593	1.202

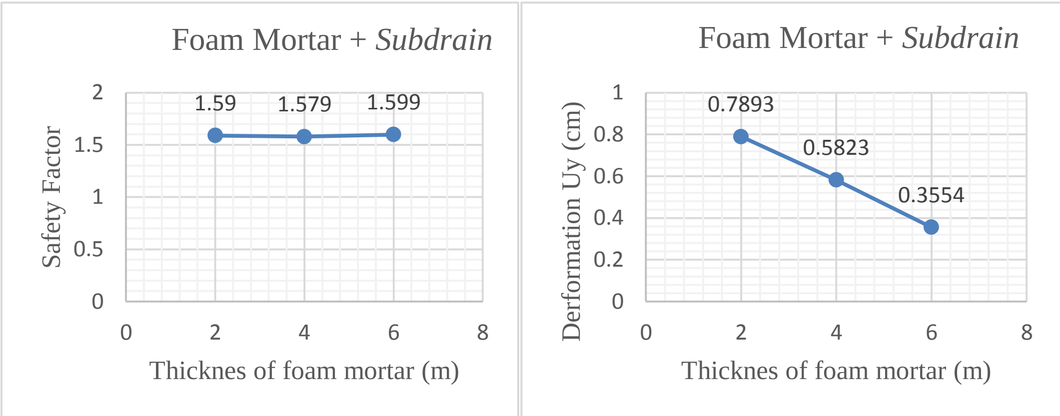

Figure 8. Graph of the Relationship Between SF, Deformations (Uy), and Foam Mortar Thickness with Subdrain

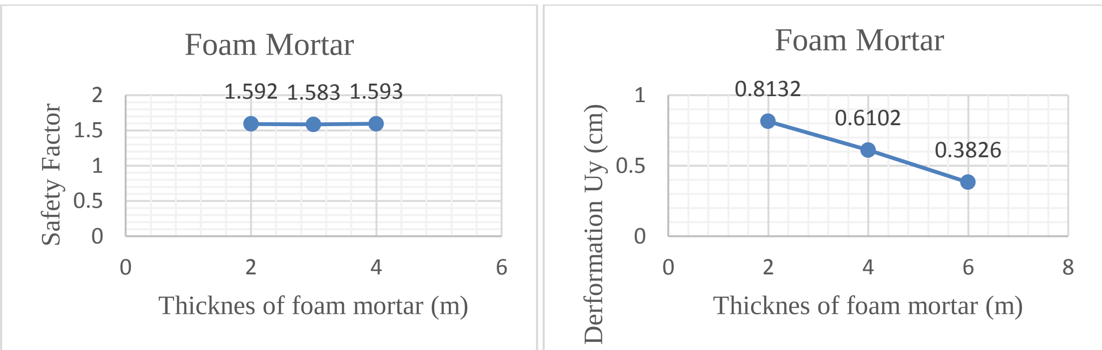

Figure 9. Graph of the Relationship Between SF, Deformations (Uy), and Foam Mortar Thickness Without Subdrain

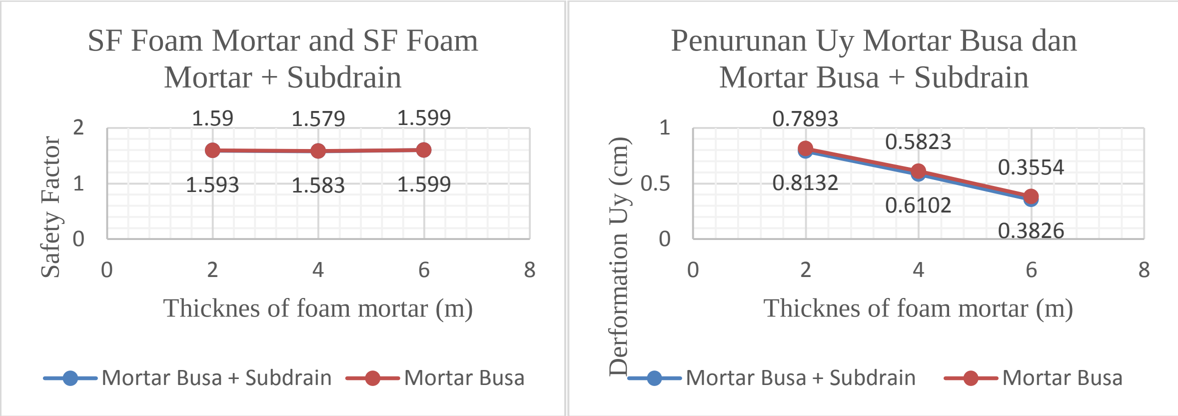

Figure 10. Graph of SF and Deformations (Uy) Comparison Using Subdrain vs. Without Subdrain for Foam Mortar Thickness Variations

The SF and deformations (Uy) results from the foam mortar reinforcement have met the required standards for both SF and deformations (Uy). The behavior of deformations (Uy) indicates that the thicker the foam mortar used, the smaller the deformations (Uy), both with and without subdrain. The smallest SF, which is 1.579, was obtained with the foam mortar reinforcement of 4m thickness with subdrain, while the largest deformations (Uy) of 0.8132 cm was observed with the 2m thick foam mortar variation without subdrain. The influence of the subdrain is shown in Figure 10, where the SF and deformations (Uy) results from the variations with and without subdrain do not show significant differences in values.

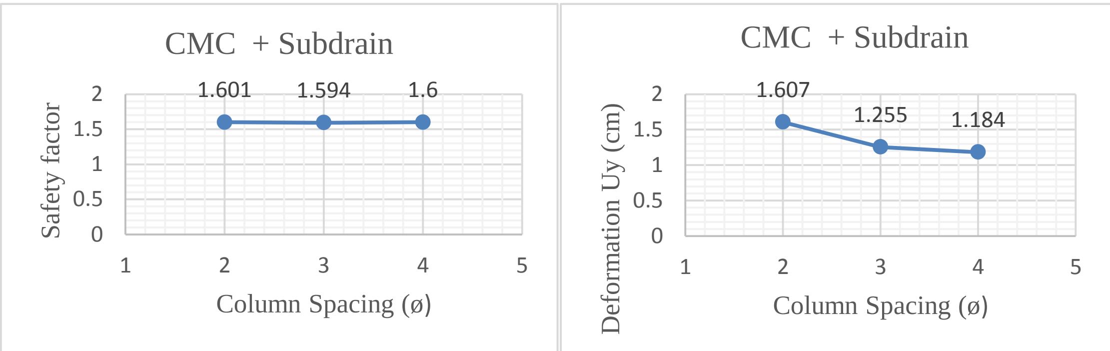

Figure 11. Graph of the Relationship Between SF, Deformations (Uy), and CMC Column Spacing with Subdrain

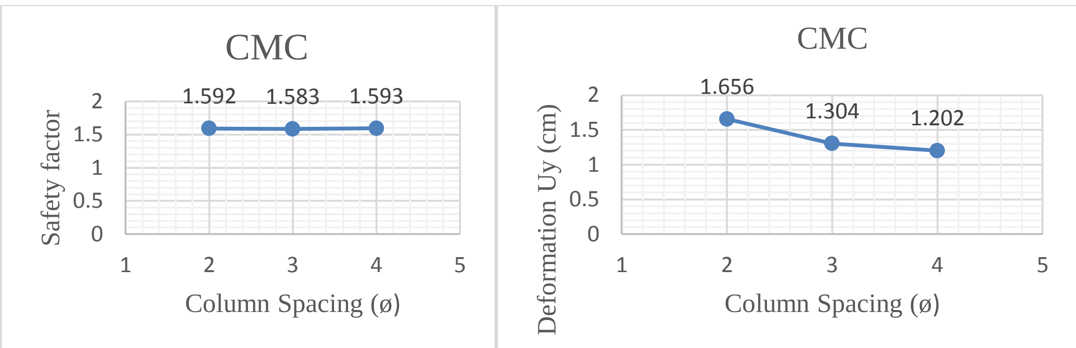

Figure 12. Graph of the Relationship Between SF, Deformations (Uy), and CMC Column Spacing without Subdrain

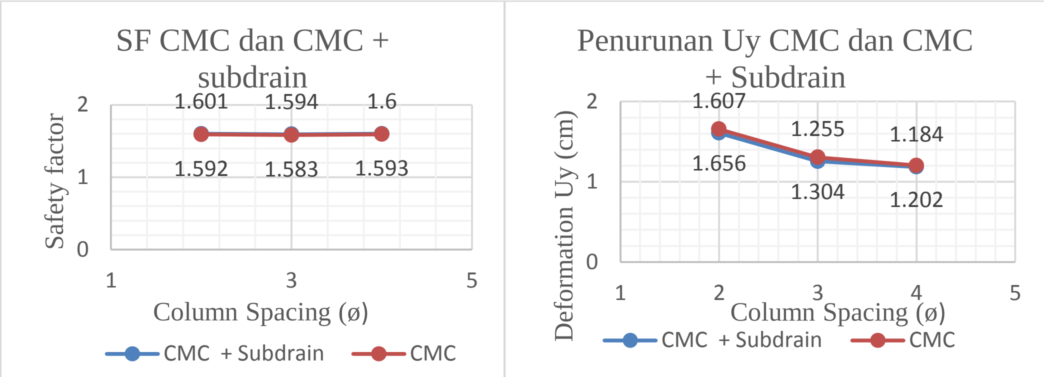

Figure 13. Graph of SF and Deformations (Uy) Comparison Using Subdrain vs. Without Subdrain for CMC Column Spacing Variations

The SF and deformations (Uy) results from the CMC reinforcement have met the required standards for both SF and deformations (Uy). The behavior of deformations (Uy) indicates that the larger the spacing between the CMC columns, the smaller the deformations (Uy), both with and without subdrain. The smallest SF, which is 1.583, was obtained with the CMC reinforcement using a 3ø column spacing without subdrain, while the largest deformations (Uy) of 1.656 cm was observed with the 2ø column spacing without subdrain. The influence of the subdrain is shown in Figure 12, where the SF and deformations (Uy) results from the variations with and without subdrain do not show significant differences in values. The Stress Reduction Ratio (SRR), as an indicator of the effectiveness of the CMC reinforcement (arching effect), was most effective with a value of 0.13, which was obtained from the 2ø column spacing without subdrain. A summary of the SRR values is shown in Table 9.

Table 9. Rangkuman nilai SRR untuk berbagai variasi jarak kolom CMC dan subdrain

Alternatif	Tebal LTP (m)	Beban Lalu Lintas (Kpa)	ɣ ltp (kN/m3)	σs (kN/m2)	σp (kN/m2)	SRR (σs/σp)
cmc 2ø with subdrain	1.2	15	17	7.706	35.4	0.22
cmc 2ø without subdrain	1.2	15	17	4.641	35.4	0.13
cmc 3ø with subdrain	1.2	15	17	17.924	35.4	0.51
cmc 3ø without subdrain	1.2	15	17	12.729	35.4	0.36
cmc 4ø with subdrain	1.2	15	17	15.953	35.4	0.45
cmc 4ø without subdrain	1.2	15	17	16.601	35.4	0.47

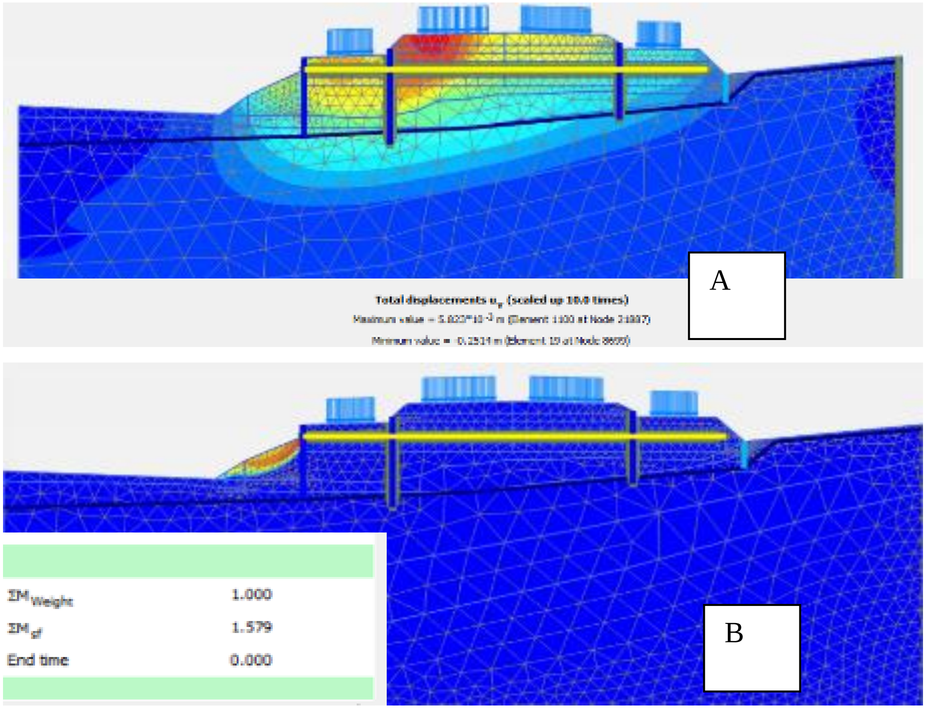

Figure 14. The example of the defromation field (Uy) and the failure surface from a Plaxis 2D output for foam mortar reinforcement with a 4m thickness and subdrain

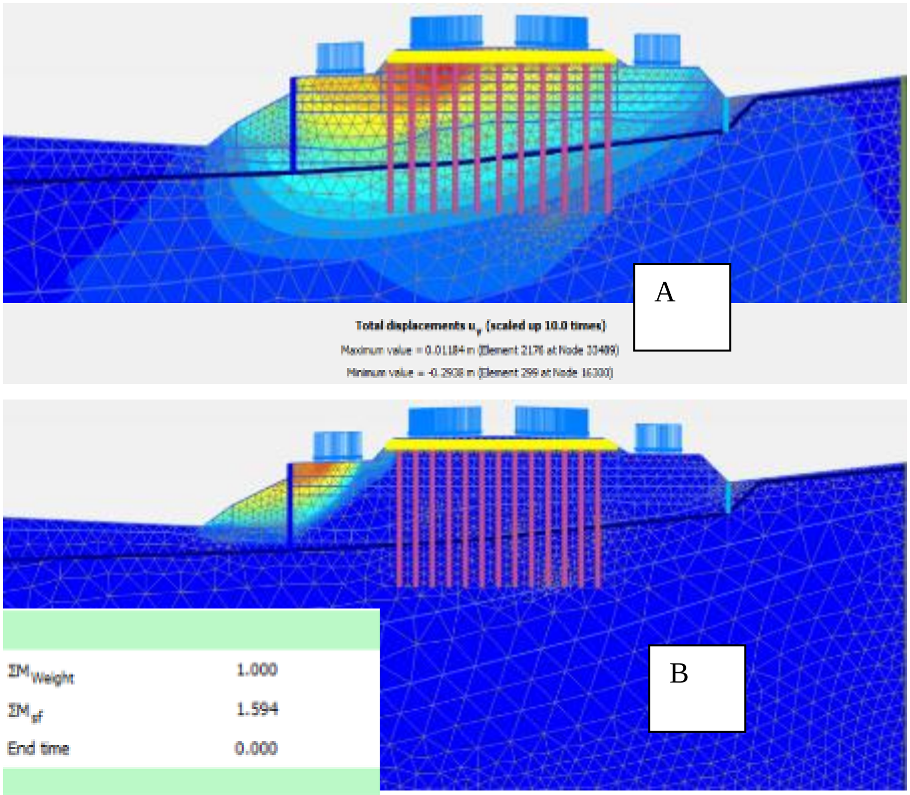

Figure 15. The example of the defromation field (Uy) and the failure surface from a Plaxis 2D output for CMC reinforcement with a 3ø column spacing with subdrain

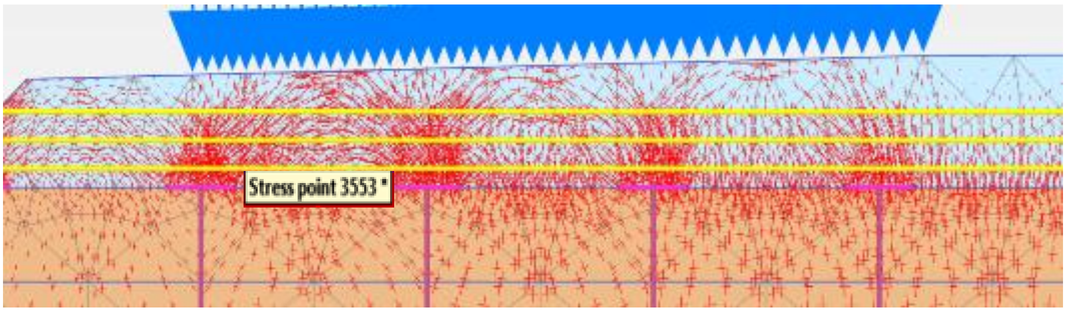

Figure 16. The arching effect formed in the context of CMC (Controlled Modulus Column) reinforcement

Figure 15 explained the stress point review locations are indicated between the CMC columns. These stress points are crucial for calculating the Stress Reduction Ratio (SRR), which is used as an indicator of the effectiveness of the arching effect.

CONCLUSIONS

Based on the initial condition analysis and the reinforcement measures that have been implemented, the following conclusions can be drawn:

1. Initial Condition: The initial SF value was 1.886 and the deformations (Uy) was 0.96 cm. This SF value did not match the actual field conditions, leading to a back-analysis, which resulted in an SF value of 0.9395 and a deformations (Uy) of 1.02 cm.
2. Foam Mortar Reinforcement: For the various foam mortar thicknesses, the smallest SF value of 1.579 was found for the 4m thick foam mortar with subdrain, while the largest deformations (Uy) of 0.8132 cm was found for the 2m thick foam mortar without subdrain.
3. CMC Reinforcement: For the various CMC configurations, the smallest SF value of 1.583 was obtained for the 3ø column spacing without subdrain, whereas the largest deformations (Uy) of 1.656 cm was found for the 2ø column spacing without subdrain.
4. Stress Reduction Ratio (SRR): The most effective SRR value, 0.13, was obtained for the 2ø column spacing without subdrain.
5. Impact of Subdrain: The subdrain did not have a significant effect because the failure surface formed was above the groundwater table. As a result, the lowering of the groundwater table due to the subdrain did not affect either the SF or the deformations (Uy).

REFERENCES

[1] Alsirawan, R. (2021). “Analysis of Embankment Supported by Rigid Inclusions Using Plaxis 3D”. *Acta Technica Jaurinensis. Vol. 14, No. 4, pp. 455-476.*

[2] Arifanto, Firman. dkk. (2024). “Analysis of Embankment Slope Failure And Effectiveness Of Reinforcement With Full Displacement Column on Soft Soil (Case Study: Construction Of Padang Sicincin Toll Road Section STA 7+400 – 7+550)”. *Journal of Infrastructure and Facility Asset Management.*

[3] Bowles, Joseph E. (1997). *Foundation Analysis And Design.* Mc Graw Hill. Singapore. New York.

[4] Das, Braja M. (2008). *Fundamental of Geotechnical Engineering Third Edition*. Chris Carson. United States of America.

[5] Das, Braja M. (2011). *Geotechnical Engineering Handbook. Florida*: J. Ross Publishing. United States of America.

[6] Eekelen, Suzane Van. (2015). "Basal Reinforced Piled Embankments Experiments, field studies and the development and validation of a new analytical design model". *Netherlands: CPI – Koninklijke Wörmann, Zutphen*.
[7] Endah, Noor. (2018). *RC 18-4712 Bahan Ajar Metode Perbaikan Tanah*. Departemen Teknik Sipil ITS. Surabaya.
[8] Hidayat, Deni. dkk. (2016). "Analisis Material Ringan Dengan Mortar Busa Pada Konstruksi Timbunan Jalan". *Seminar Nasional Sains dan Teknologi 2016*.
[9] Moulton, Lyle K. (1980). *Highway Subdrainage Design*. Federal Highway Administration. Washington D.C.
[10] SNI 8460:2017. *SNI 8460:2017tentamg Persyaratan Perancangan Geoteknik.*
[11] Wartoyo, Lalu A. dkk. (2022). "Analisis Stabilitas Timbunan Tinggi Pada Mortar Busa Menggunakan Metode Elemen Hingga Pada Proyek Pembangunan Jalan Baru Batas Kota Singaraja – Mengwitani". *Jurnal Aplikasi Teknik Sipil Volume 20, Nomor 1*.
[12] 42/SE/M/2015. *Surat Edaran Menteri Pekerjaan Umum dan Perumahan Rakyat Tahun 2015 Perencanaan teknis timbunan material ringan mortar-busa untuk konstruksi jalan*.